

# RPA susceptibility of the superconducting layered transition metal oxide $\text{Li}_x\text{NbO}_2$

E. R. Ylvisaker and W. E. Pickett  
*University of California, Davis*  
(Dated: May 17, 2011)

The  $\text{Li}_x\text{NbO}_2$  system, synthesized and found to be superconducting (around 5 K) soon after the high  $T_c$  cuprates were discovered, is another example of a quasi-two-dimensional, effective single-band transition metal oxide insulator that superconducts when doped, and has the additional interest of its hexagonal lattice. Earlier dynamical mean field study by Lee *et al.*<sup>1</sup> showed that  $x = 0$   $\text{NbO}_2$  is near if not at a Mott insulating condition, so superconducting  $\text{Li}_x\text{NbO}_2$  can be considered a heavily electron-doped Mott insulator or a moderately hole-doped band (ionic) insulator). Though the Fermi surface and Fermi level density of states  $N(E_F)$  change considerably, the superconducting critical temperature  $T_c \approx 5$  K remains nearly doping independent in the range  $0.45 < x < 0.8$ , and vanished for  $x > 0.8$ . To study possible mechanisms of pairing, we extend the random phase approximation to include long range (intersite) interactions ( $V$ ) in addition to the on-site repulsion ( $U$ ), and evaluate both the spin ( $\chi^S$ ) and charge ( $\chi^C$ ) susceptibilities. For the chosen values of  $U$  and  $V$ , the variation with  $\mathbf{q}$  of the macroscopic (volume averaged) susceptibility with doping correlates with changes in the Fermi surface over the experimentally accessible doping range. Peaks in  $\chi^C$  always occur at the zone corner point K, consistent with tendencies (but weak ones) to charge order on neighboring sites. The  $\mathbf{q}$  dependence of  $\chi^S$  shows more variation with doping level.

## I. INTRODUCTION

The high  $T_c$  cuprate superconductors (HTS), with their quasi-two dimensional crystal and electronic structure and proximity to a magnetically ordered insulating phase, redirected the attention to mechanisms of superconducting pairing from phonon-coupled to magnetically mediated. The role of the two dimensionality itself is unclear, and the recent discovery of high temperature superconductivity in the iron pnictide superconductors adds more examples into the discussion. Additionally, other layered transition metal oxides that become superconducting when doped ( $\text{Li}_x\text{NbO}_2$ ,  $\text{Na}_x\text{CoO}_2$ ) have been discovered and studied to varying degrees. These systems are of course different from cuprates and the iron pnictides: the transition metal lattice is hexagonal, not square, and  $T_c$  is around 5 K rather than 50-100 K.

Not long after the 1986 discovery of high temperature superconductivity in the layered cuprates, superconductivity with  $T_c \approx 5$  K was discovered<sup>2</sup> in the layered niobate  $\text{Li}_x\text{NbO}_2$ , at  $x = 0.45$  and  $0.50$ . Since then the superconductivity has been confirmed within  $0.45 < x < 0.79$  without any significant variation of  $T_c$ .<sup>2-5</sup> No superconductivity has been found in the weakly doped regime of  $1 > x > 0.84$ .<sup>4</sup> Hall effect measurements have confirmed charge carriers are hole-like,<sup>6</sup> consistent with  $\text{Li}_x\text{NbO}_2$  being a hole-doped band insulator.  $\text{Li}_x\text{NbO}_2$  might be superconducting for  $x < 0.45$ , however there may be difficulty in the synthesis at such a low Li concentration due to the considerable covalency of Li along  $c$ -direction, as evidenced our previously calculated Born effective charges of  $\text{LiNbO}_2$ .<sup>7,8</sup> Additionally, the  $x = 0$   $\text{NbO}_2$  system is structurally distinct from the hexagonal  $\text{Li}_x\text{NbO}_2$  system, which may present additional difficulties in synthesizing hexagonal  $\text{Li}_x\text{NbO}_2$  with low  $x$ .

There are two interesting related materials, the

isostructural  $\text{Na}_x\text{NbO}_2$  and the relatively unstudied  $\text{H}_x\text{LiNbO}_2$ . The superconducting transition for  $\text{Na}_x\text{NbO}_2$  has been observed to be slightly lower than for  $\text{Li}_x\text{NbO}_2$ , with  $T_c \approx 4$  K.<sup>9,10</sup> If the replacement of Li with Na is interpreted as an isotope substitution, then the isotope shift  $\alpha = -\Delta(\ln T_c)/\Delta(\ln M) = 0.27$ , consistent with phonon-mediated pairing with strong involvement of the alkali ion. Since this replacement involves some (ion size related) structural change, the isotope effect interpretation is not certain. Even so, one would not expect there to be strong electron-phonon coupling with the alkali ion, based on analogous superconductors such as intercalated graphite. Systematic isotope studies on the substitution of Nb or O have not been done.  $\text{H}_x\text{LiNbO}_2$  shows<sup>11</sup> superconductivity with  $T_c = 5$  K at  $x = 0.3$  and  $0.5$ . If the intercalation of H has the same effect as the de-intercalation of Li, then this would suggest H enters the lattice as  $\text{H}^-$ . However due to lack of structural or systematic doping studies of  $\text{H}_x\text{LiNbO}_2$ , the role H plays is not understood.

The superconducting mechanism of  $\text{Li}_x\text{NbO}_2$  has received little attention so far. Experimental measurements<sup>5</sup> of the specific heat for  $x = 0.68$  suggest that it is an  $s$ -wave superconductor. Additionally, the linear specific heat coefficient  $\gamma_{exp} = 3.59$  mJ/mol K<sup>2</sup> and the Debye temperature 462 K were obtained. The virtual crystal approximation (Li nuclear charge  $Z = 2 + x$ ), leads to the band structure value  $\gamma_b = 2.43$  mJ/mol K<sup>2</sup> at  $x = 0.68$ , corresponding to weak electron-phonon coupling strength  $\lambda = \frac{\gamma_{exp}}{\gamma_b} - 1 \approx 0.48$ , which might however be enough to account for  $T_c \approx 5$  K. The electron-phonon mechanism is consistent with stated theoretical viewpoints,<sup>7,12</sup> however unanswered questions remain. Within the superconducting range ( $0.45 < x < 0.8$ ) the transition temperature remains nearly constant at 5 K, however in a rigid band model the density of states (shown in Fig. 1) varies by a factor of 2 over that same

range. Our previous theoretical work<sup>7,8</sup> found evidence of strong electron-phonon coupling to the Raman active vibrational motion of the O atoms. The strong electron-phonon coupling to a few phonons could explain the superconductivity of  $\text{Li}_x\text{NbO}_2$ , similarly to  $\text{MgB}_2$ , but a more thorough investigation to see if this is the case has yet to be done.

On the other hand, as a transition metal oxide with rather small bandwidth, one can envision  $\text{Li}_x\text{NbO}_2$  in a localized sense as a  $(1-x)|d^1\rangle + x|d^2\rangle$  system, in which charge and spin fluctuations may assume a dominant role. This view is consistent with the observation that  $\text{Li}_x\text{NbO}_2$  is not conducting for  $x > 0.84$ , and is also in line with a dynamical mean field theory study showing that the  $x=0$  end compound is near, if not at, a Mott insulating condition, making it further resemble the cuprate high temperature superconductors. In one popular scenario for the cuprates, a strong peak in the spin susceptibility near  $(\pi, \pi)$  provides the mechanism for  $d$ -wave pairing. In this work we examine the spin and charge susceptibilities of  $\text{Li}_x\text{NbO}_2$  in a large range of  $x$  within the random phase approximation (RPA), to identify possible signatures of interest in this superconductor.

## II. RPA FORMALISM

The RPA begins by applying perturbation theory to a non-interacting electron gas with a Hubbard Hamiltonian as a perturbation. Here we will consider the non-interacting Hamiltonian as

$$H_0 = \sum_{\mathbf{k}, ab} H_{ab}^{\mathbf{k}} c_{\mathbf{k},a}^\dagger c_{\mathbf{k},b} \quad (1)$$

where  $\mathbf{k}$  is a (pseudo-)momentum value,  $a$  and  $b$  are composite spin/orbital indices for some localized tight-binding basis. Hereafter, we assume that  $H_{ab}^{\mathbf{k}}$  independent of the spins of  $a$  and  $b$ , excepting that it is diagonal in spin (ie. it's a paramagnetic Hamiltonian with no spin-orbit coupling). We start with a general interacting Hamiltonian of

$$H_1 = \frac{1}{2} \sum_{\substack{abcd \\ n}} U_{abcd} c_{na}^\dagger c_{nb} c_{nc}^\dagger c_{nd} \\ + \sum_{\substack{abcd \\ \langle n,m \rangle}} V_{abcd} c_{na}^\dagger c_{nb} c_{mc}^\dagger c_{md} \quad (2)$$

where the sum over  $n$  runs over sites in the lattice, and the sum over  $\langle n, m \rangle$  runs over bonds to near neighbors, although the generalization to further neighbors will be readily apparent. We assume  $U$  and  $V$  to be symmetric and real, that is  $U_{abcd}^* = U_{abcd} = U_{cdab}$ . The Fourier transform of the interaction is

$$H_1 = \frac{1}{2N} \sum_{\substack{abcd \\ \mathbf{k}\mathbf{p}\mathbf{q}}} F_{abcd}^{(\mathbf{q})} c_{\mathbf{k},a}^\dagger c_{\mathbf{k}+\mathbf{q},b} c_{\mathbf{p}+\mathbf{q},c}^\dagger c_{\mathbf{p},d} \quad (3)$$

where  $F_{abcd}^{(\mathbf{q})} = U_{abcd} + \gamma(\mathbf{q})V_{abcd}$  and  $\gamma(\mathbf{q}) = \sum_l e^{i\mathbf{q}\cdot\mathbf{R}_l}$  is the structure factor, with  $l$  running over  $m-n$ .

### A. Susceptibility

The spin and charge susceptibilities are defined as

$$\chi_{abcd}^{S,C}(\tau, \mathbf{q}) = \left\langle \left( p_{ab\uparrow}(\tau, \mathbf{q}) \pm p_{ab\downarrow}(\tau, \mathbf{q}) \right) \right. \\ \left. \times \left( p_{cd\uparrow}^\dagger(0, \mathbf{q}) \pm p_{cd\downarrow}^\dagger(0, \mathbf{q}) \right) \right\rangle \quad (4)$$

using the orbital excitation creation operator is

$$p_{ab\sigma}^\dagger(\tau, \mathbf{q}) = \sum_{\mathbf{k}} c_{\mathbf{k}+\mathbf{q},a\sigma}^\dagger(\tau) c_{\mathbf{k},b\sigma}(\tau).$$

with the charge (spin) susceptibility taking the plus (minus) sign. Note that in Eq. 4 that  $a, b, c, d$  represent just orbital indices.

### B. Parametrizing the interaction

So far, we have defined a general susceptibility for a rather arbitrary interaction. To make this useful, we consider a specific form of the interaction with a few parameters. Following previous works<sup>13</sup> we will use four parameters to define the on-site interaction. In addition to this, we use two parameters to define the intersite interaction. The interacting Hamiltonian in real space are then given by the sum of two contributions,

$$H_1^{\text{on-site}} = \sum_n \left[ \sum_a U_a c_{na\uparrow}^\dagger c_{na\uparrow} c_{na\downarrow}^\dagger c_{na\downarrow} \right. \\ \left. + \sum_{a\sigma \neq b\sigma'} \frac{1}{2} U'_{a,b} c_{na\sigma}^\dagger c_{na\sigma} c_{nb\sigma'}^\dagger c_{nb\sigma'} \right]. \\ H_1^{\text{intersite}} = \sum_{n,m} \sum_{a\sigma, b\sigma'} \frac{1}{2} V_{an,bm} c_{na\sigma}^\dagger c_{na\sigma} c_{mb\sigma'}^\dagger c_{mb\sigma'} \quad (5)$$

The parameters  $U$  and  $U'$  are the standard intraorbital and interorbital Coulomb repulsion that is used in applications of the Hubbard model elsewhere. For long range interactions, we include a density-density Coulomb repulsion  $V$ . The factor of  $\frac{1}{2}$  in the intersite interaction accounts for the double counting of pairs in the summation over  $n$  and  $m$ .

We can write the spin and charge susceptibilities as

$$\chi^S(\omega, \mathbf{q}) = [1 - S(\mathbf{q})\chi^0(\omega, \mathbf{q})]^{-1} \chi^0(\omega, \mathbf{q}) \quad (6a)$$

$$\chi^C(\omega, \mathbf{q}) = [1 + C(\mathbf{q})\chi^0(\omega, \mathbf{q})]^{-1} \chi^0(\omega, \mathbf{q}) \quad (6b)$$

with the matrix multiplication carried out by contracting the first and last pair of orbital indices as separate matrix indices. The bare susceptibility is obtained from

the standard expressions

$$\chi_{abcd}^0(\omega) = \sum_{\mathbf{k}} G_{ad}(\mathbf{k}, \omega) G_{cb}(\mathbf{k} + \mathbf{q}, \omega), \quad (7a)$$

$$G_{ab}(\mathbf{k}, \omega) = \sum_n \frac{\langle a|\mathbf{k}n\rangle \langle \mathbf{k}n|b\rangle}{\omega + \mu - \varepsilon_{\mathbf{k}n}}. \quad (7b)$$

The spin and charge matrices are defined as

$$S_{abcd}^{(\mathbf{q})} = \begin{cases} U_a, & a = b = c = d \\ U'_{ab}, & a = c \neq b = d \end{cases} \quad (8)$$

$$C_{abcd}^{(\mathbf{q})} = \begin{cases} U_a + V_{ac}(\mathbf{q}), & a = b = c = d \\ -U'_{ab}, & a = c \neq b = d \\ 2U'_{ac} + V_{ac}(\mathbf{q}), & a = b \neq c = d \end{cases}$$

where  $V_{ac}(\mathbf{q}) \equiv V_{ac} \text{Re} \gamma(\mathbf{q})$ .

The susceptibilities described so far contain orbital indices. The experimentally observable susceptibility, hereafter referred to as the macroscopic susceptibility, can be derived similarly via perturbation theory<sup>14</sup> and related to Eqs. 6 via

$$\chi^{S,C}(\mathbf{q}) = \sum_{a,b} \chi_{aa,bb}^{S,C}(\mathbf{q}). \quad (9)$$

### III. CALCULATED SUSCEPTIBILITIES

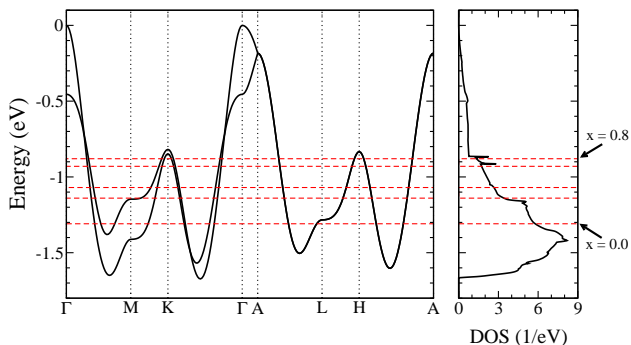


FIG. 1. Band structure (left panel) and density of states (right panel) for  $\text{Li}_x\text{NbO}_2$ . Dashed horizontal lines indicate rigid band doping from the bottom up for  $x = 0$ ,  $x = 0.5$ ,  $x = 0.6$ ,  $x = 0.75$  and  $x = 0.8$ . For  $x > 0.8$  there are no Fermi surfaces around the K point, and the bands are completely filled for  $x = 1$ , giving a band insulator.

$\text{Li}_x\text{NbO}_2$  is a rare example of a single band system in a real materials, and has the additional interest of a hexagonal lattice (which is frustrated for antiferromagnetic interactions). We begin, as conventional, with the local density approximation (LDA) band structure and Bloch wavefunctions, and consider the effects of residual interactions as discussed in the previous section.

We construct symmetry projected Wannier functions using density functional theory with the FPLO code,<sup>15</sup> with symmetry projections as described in Ref. 7. The

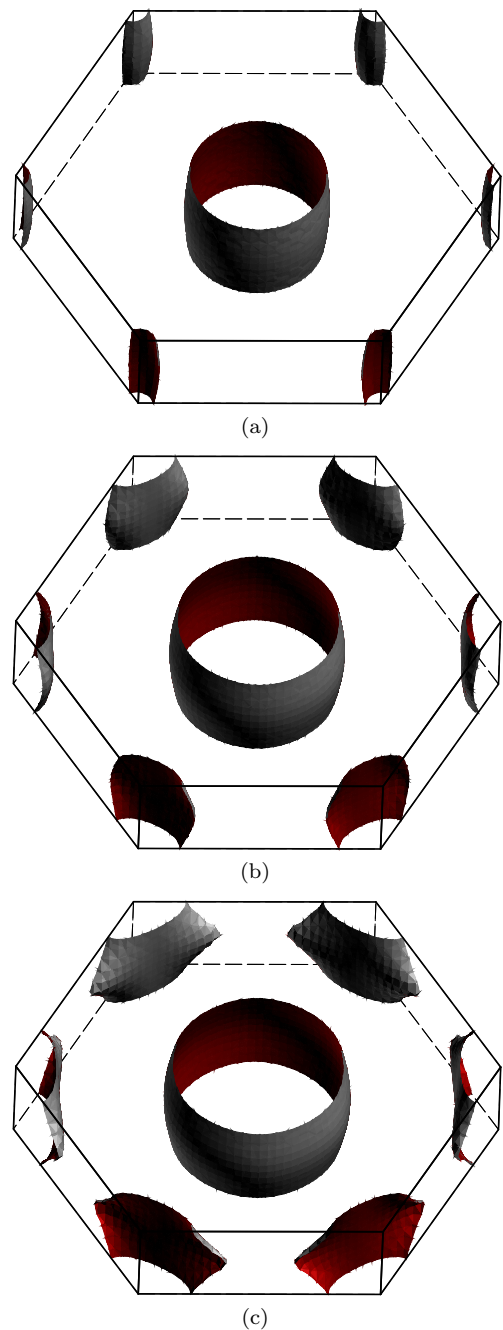


FIG. 2. Fermi surfaces for (a)  $E_F = -0.88$ , (b)  $E_F = -1.07$ , and (c)  $E_F = -1.14$  measured relative to the top of the band. These correspond to approximately (a)  $x = 0.8$ , (b)  $x = 0.6$  and (c)  $x = 0.5$ . For clarity, only the larger of the two Fermi surfaces is shown (both are very similar). The surfaces are colored by the velocities  $v_{\mathbf{k}} = |\nabla_{\mathbf{k}} \varepsilon_{\mathbf{k}}|$ .

non-interacting Hamiltonian that we have used is constructed via a tight-binding representation with these Wannier functions as basis functions, which reproduces the LDA bands excellently. Computation of the susceptibilities was carried out using a fine  $\mathbf{k}$ -mesh of  $120 \times 120 \times 10$ . A finite temperature Fermi-Dirac distribution is used

to smear occupations and achieve converged results for the summation over  $\mathbf{k}$ . An inverse temperature of  $\beta = 100\text{eV}^{-1}$  was used.

The triangular prismatic coordination of Nb on the triangular lattice separates the  $d_{z^2}$  orbital from the other higher lying ones, making the corresponding band the only one of interest. Thus this is a single band system (complicated slightly by having two formula units in the crystallographic primitive cell as a result of the stacking of  $\text{NbO}_2$  layers). Lithium doping changes the carrier concentration in the Nb  $4d_{z^2}$  band, according to  $(\text{Li}^+)_x\text{Nb}^{+Q}\text{O}^{-2}$  the Nb  $4d$  formal charge state is  $Q = +4 - x$ , corresponding to  $d^{1+x}$  occupation.

### A. Change of electronic structure with doping

Within the rigid band picture, the density of states (DOS) in states/eV-unit cell (two formula units) at the Fermi level varies from  $N(E_F) = 1.4$  at  $x = 0.8$  down to 3.6 at  $x = 0.5$ , while the observed  $T_c$  does not change appreciably in this range. Above  $x = 0.8$  there is a sharp drop in the DOS. From examination of the band structure in Fig. 1 this is seen to be due a Lifshitz transition where the Fermi surfaces around the K point disappear at higher  $x$ . It seems likely then that these K-point Fermi surfaces have an important connecton to the superconductivity, however it is puzzling (for any mechanism) that  $T_c$  is insensitive to  $N(E_F)$  and the size of these Fermi surfaces. For doping levels of interest the progression of the Fermi surfaces is shown in Fig. 2.

Below  $x = 0.5$  there is a sharp increase in the DOS from the van Hove singularity occuring at the flat region of the bands near M. The Fermi surfaces around the two K points begin to merge into a single large Fermi surface at this point. The increase in  $N(E_F)$  below this doping may promote a structural instability, which could explain the transition away from the trigonal prismatic structure and identify the lowest experimentally realizable doping for  $\text{Li}_x\text{NbO}_2$ . At  $x = 0$ ,  $\text{NbO}_2$  is a rutile structure with a rather three dimensional electronic structure,<sup>16</sup> unlike the quasi-2D bands of hexagonal  $\text{Li}_x\text{NbO}_2$ .

### B. RPA Spin and Charge Susceptibilities

The interaction parameters we chose are  $U = 0.3$  eV for the on-site repulsion, and  $V = 0.15$  eV for nearest neighbor repulsion. Since RPA tends to overestimate the effect of correlations due to the lack of a self-energy correction to the band structure,<sup>13</sup> these values are chosen to be somewhat smaller than would otherwise be used. The ratio  $U/V = 2$  may seem somewhat small, but we believe this is justified due to the significant delocalization of the Wannier function which describes these bands.<sup>7</sup> These values are chosen so that at  $x = 0$  where the bare susceptibility is the largest, the charge susceptibility is nearly divergent at inverse temperature  $\beta = 100$ .

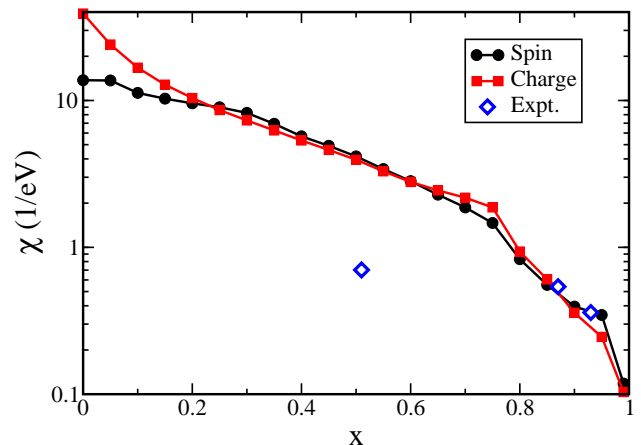


FIG. 3. Maximum value with respect to  $\mathbf{q}$  of the macroscopic spin and charge susceptibilities  $\chi^{S,C}(\mathbf{q})$  of  $\text{Li}_x\text{NbO}_2$  plotted against the doping level  $x$ . As  $x$  goes to 1, the system becomes a band insulator and the susceptibilities go to zero. The kink at  $x = 0.75$  is due to the Lifshitz transition described in the text. Blue diamonds are scaled experimental magnetic susceptibilities from Ref. 17.

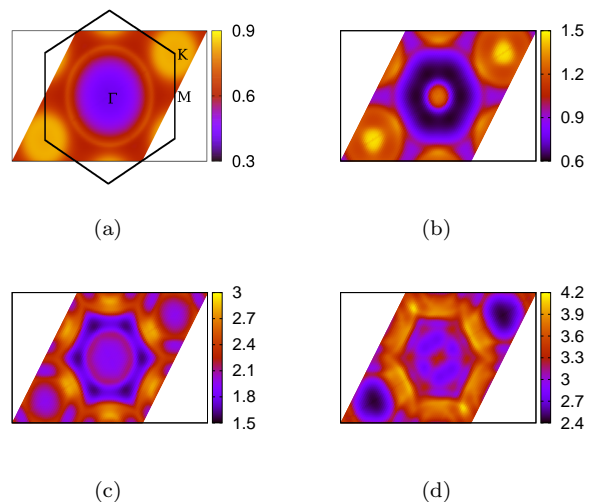


FIG. 4. RPA spin susceptibility in the  $k_z = 0$  plane of the triangular Brillouin zone for (a)  $x = 0.80$ , (b)  $x = 0.75$ , (c)  $x = 0.60$ , (d)  $x = 0.50$ . Color bars are in units of  $(1/\text{eV})$ . The hexagonal Brillouin zone is shown in (a), with the  $\Gamma$  point at the center of each figure, the K point at the corner, the M point in the center of each line. An area of one full Brillouin zone is shown, although not in the conventional hexagonal shape.

The maximum values of the spin and charge susceptibilities are shown as a function of doping in Fig. 3. There is very little experimental data on the susceptibility of  $\text{Li}_x\text{NbO}_2$ , with only three data points coming from Ref. 17. Of particular note is the sudden change in the slope of the calculated susceptibilities vs.  $x$  near  $x = 0.75$ , which correlates with the Lifshitz transition that occurs near that doping and lies near the upper range of observed

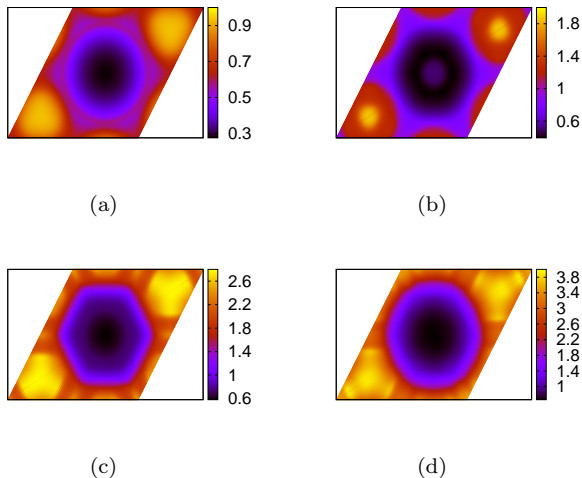


FIG. 5. RPA charge susceptibility in the  $k_z = 0$  plane of  $\text{Li}_x\text{NbO}_2$  for (a)  $x = 0.80$ , (b)  $x = 0.75$ , (c)  $x = 0.60$ , (d)  $x = 0.50$ . The peaks in the corners occur at the two K points in the Brillouin zone.

superconductivity.

### 1. Spin susceptibility

RPA spin susceptibilities as a function of  $\mathbf{q}$  in the Brillouin zone for selected values of  $x$  in the range 0.5-0.8 are shown in Figs. 4. At  $x = 0.8$  (Fig. 4a) there is a broad incoherent feature around each of the two K points in the Brillouin zone. These broad features are due to scattering from states just below the Fermi level around K to states near the Fermi surface surrounding  $\Gamma$ . A ring of local maximum of intensity circles  $\Gamma$  at a radius of  $2k_F$ , reflecting scattering across the circular Fermi surface (or radius  $k_F$ ).

Decreasing  $x$  to 0.75 (Fig. 4b) results in several changes. The maxima at the K points intensifies and narrows, and a ring of maximum encircles these K points. Such a circular ring is expected to arise at a non-zero momentum  $Q$  when there are circular Fermi surfaces separated by  $Q$ , which is the case here:  $Q$  happens to be this same momentum K. The circular features surrounding  $\Gamma$  from scattering within within a circular Fermi surfaces are not so evident, apparently due to overlap of features resulting from scattering within the Fermi surfaces centered at K and those centered at  $\Gamma$ . A narrow local maximum has appeared at  $\Gamma$ .

As  $x$  is decreased further to  $x = 0.6$  (Fig. 4c), new incommensurate peaks appear, as the Fermi surface topology is close to a significant change where cylinders around K distort and begin to touch at the M point (in the  $k_z = 0$  plane). These incommensurate peaks surely have contributions that come from scattering near  $\Gamma$  to near M. At  $x = 0.5$  the incommensurate peaks in  $\chi^S$  become broader, and appear organized into into overlap-

ping structures centered at the K points.

### 2. Charge susceptibility

The charge susceptibilities, shown in Fig. 5 are always peaked around the K points, which corresponds to the tendency for charge alternation on neighboring Nb ions. This incipient charge order corresponds to the charge density wave that is observed in  $2\text{H-TaSe}_2$ , which is isostructural and isoelectronic with  $\text{Li}_x\text{NbO}_2$  at  $x = 0$ . The use of a near neighbor interaction introduces a structure factor into the RPA calculation which will always favor this ordering vector. However, as seen in Figs. 5, this peak is broad for several values of  $x$ , though it narrows very significantly for  $x=0.75$ . For the value of  $V/U$  that we have used, the peak at K is not particularly strong.

## IV. CONCLUDING REMARKS

In this paper we have used a density functional derived single particle Hamiltonian, with on-site and intersite repulsive interactions, to calculate the bare and RPA spin and charge susceptibilities for  $\text{Li}_x\text{NbO}_2$  in the range of doping where superconductivity is observed. This approach provides a beginning on the question of how spin and charge fluctuations interfere with, and compete with, electron-phonon coupling in providing the pairing mechanism for the observed superconductivity. The strongly two dimensional, doped transition metal oxide character of this system puts it into the class that contains the high temperature superconducting cuprates.

We find that the  $\mathbf{q}=0$  spin and charge susceptibilities are nearly the same magnitude over the range  $0.2 < x < 0.75$ . Incoherent (*i.e.* rather broad) peaks in the susceptibility suggest that the charge and spin fluctuations do not cause a strong tendency to order in this system. The growth in the susceptibility as  $x$  is decreased correlates with the growth in the density of states, so if these fluctuations suppress the phonon-mediated superconductivity such as was indicated by Rietschel<sup>18,19</sup> in some detail, this may help to explain why the superconducting transition temperature does not deviate significantly from 5 K in all reported measurements.

There are several systems where order (charge density waves [CDW] or spin density waves [SDW]) inhibit superconductivity (hence the characterization as *competing*) yet when this order disappears but the fluctuations remain, superconductivity immediately appears. Several transition metal dichalcogenides fit into this category, with  $\text{Cu}_x\text{TaS}_2$  [20] with its CDW behavior providing a recent example. With its structural and compositional similarity to  $\text{Li}_x\text{NbO}_2$ , there is reason to look for common underlying mechanisms. As for the effects of spin fluctuations, Scalapino has provided an overview of theoretical developments in the understanding of such competition through the end of the last century.<sup>21</sup> Heavy

fermion superconductivity brought additional focus on magnetic pairing mechanisms<sup>22</sup> and the high temperature superconducting cuprates intensified that viewpoint, but  $\text{Li}_x\text{NbO}_2$  seems nowhere near either of those two regimes.

It is worth recounting a few more aspects of our results. The  $\mathbf{q}$ -dependence of the spin susceptibility shows strong variation in the range  $0.5 < x < 0.8$ . The change in the charge susceptibility is somewhat less, with the main difference being the width of the peak at the K points. The maxima in both susceptibilities increases in strength as half-filling ( $x = 0$ ) is approached. In contrast to this variation, the observed critical temperature is almost independent of doping level. It is reasonable to conclude that, if superconductivity in  $\text{Li}_x\text{NbO}_2$  is due to spin or charge fluctuations, the lack of strong variation in the momentum distribution of these fluctuations puts  $\text{Li}_x\text{NbO}_2$  in

a class distinct from those where competition between superconductivity and CDWs, or SDWs, are observed to occur. The calculated sensitivity of doped  $\text{Li}_x\text{NbO}_2$  to the oxygen positions<sup>7</sup> leads to topological changes in the Fermi surface as the oxygen  $z$  position is varied. This sensitivity to lattice displacement can be interpreted as indicating the superconductivity is phonon-mediated and furthermore, is related to the Lifshitz transition that occurs near  $x = 0.8$  when cylindrical Fermi surfaces (reminiscent of  $\text{MgB}_2$ ) begin to appear.

## V. ACKNOWLEDGMENTS

We acknowledge funding from DOE grant DE-FC02-06ER25794 and conversations with R. T. Scalettar and Q. Yin.

- 
- <sup>1</sup> K.-W. Lee, J. Kuneš, R. T. Scalettar, and W. E. Pickett, *Phys. Rev. B* **76**, 144513 (2007).
- <sup>2</sup> M. J. Geselbracht, T. J. Richardson, and A. M. Stacy, *Nature* **345**, 324 (1990).
- <sup>3</sup> P. Bordet, E. Moshopoulou, S. Liesert, and J. J. Capponi, *Physica C* **235-240**, 745 (1994).
- <sup>4</sup> E. G. Moshopoulou, P. Bordet, and J. J. Capponi, *Phys. Rev. B* **59**, 9590 (1999).
- <sup>5</sup> G. T. Liu, J. L. Luo, Z. Li, Y. Q. Guo, N. L. Wang, D. Jin, and T. Xiang, *Phys. Rev. B* **74**, 012504 (2006).
- <sup>6</sup> D. G. Kellerman, G. P. Shveikin, A. P. Tyutyunnik, V. G. Zubkov, V. A. Perelyaev, T. V. D'yachkova, N. I. Kadyrova, A. S. Fedyukov, S. A. Turzhevskii, V. A. Gubanov, et al., *Superconductivity:Phys. Chem. Tech.* **5**, 2035 (1992).
- <sup>7</sup> E. R. Ylvisaker and W. E. Pickett, *Phys. Rev. B* **74**, 075104 (2006).
- <sup>8</sup> E. R. Ylvisaker, K.-W. Lee, and W. E. Pickett, *Physica B* **383**, 63 (2006).
- <sup>9</sup> D. G. Kellerman, V. G. Zubkov, A. P. Tyutyunnik, V. S. Gorshkov, V. A. Perelyaev, G. P. Shveikin, S. A. Turzhevskii, V. A. Gubanov, and A. E. Kafkin, *Superconductivity:Phys. Chem. Tech.* **5**, 966 (1992).
- <sup>10</sup> A. P. Tyutyunnik, V. G. Zubkov, D. G. Kellerman, V. A. Perelyaev, A. E. Kafkin, and G. Svensson, *Eur. J. Solid State Inorg. Chem.* **33**, 53 (1996).
- <sup>11</sup> N. Kumada, S. Watauchi, I. Tanaka, and N. Kinomura, *Mater. Res. Bull.* **35**, 1743 (2000).
- <sup>12</sup> D. L. Novikov, V. A. Gubanov, V. G. Zubkov, and A. J. Freeman, *Phys. Rev. B* **49**, 15830 (1994).
- <sup>13</sup> K. Kuroki, H. Usui, S. Onari, R. Arita, and H. Aoki, *Phys. Rev. B* **79**, 224511 (2009).
- <sup>14</sup> J. F. Janak, *Phys. Rev. B* **16**, 255 (1977).
- <sup>15</sup> K. Koepf and H. Eschrig, *Phys. Rev. B* **59**, 1743 (1999).
- <sup>16</sup> M. Posternak, A. J. Freeman, and D. E. Ellis, *Phys. Rev. B* **19**, 6555 (1979).
- <sup>17</sup> N. Kumada, S. Muramatsu, F. Muto, N. Kinomura, S. Kikkawa, and M. Koizumi, *J. Solid State Chem.* **73**, 33 (1988).
- <sup>18</sup> H. Rietschel and H. Winter, *Phys. Rev. Lett.* **43**, 1256 (1979).
- <sup>19</sup> H. Rietschel, *Phys. Rev. B* **24**, 155 (1981).
- <sup>20</sup> K. E. Wagner, E. Morosan, Y. S. Hor, J. Tao, Y. Zhu, T. Sanders, T. M. McQueen, H. W. Zandbergen, A. J. Williams, D. V. West, et al., *Phys. Rev. B* **78**, 104520 (2008).
- <sup>21</sup> D. J. Scalapino, *J. Low Temp. Phys.* **117**, 179 (1999).
- <sup>22</sup> D. J. Scalapino, E. Loh, and J. E. Hirsch, *Phys. Rev. B* **34**, 8190 (1986).